FIRST HITTING TIME OF A ONE-DIMENSIONAL LÉVY FLIGHT TO SMALL TARGETS*

DANIEL GOMEZ[†] AND SEAN D. LAWLEY[‡]

Abstract. First hitting times (FHTs) describe the time it takes a random "searcher" to find a "target" and are used to study timescales in many applications. FHTs have been well-studied for diffusive search, especially for small targets, which is called the narrow capture or narrow escape problem. In this paper, we study the FHT to small targets for a one-dimensional superdiffusive search described by a Lévy flight. By applying the method of matched asymptotic expansions to a fractional differential equation we obtain an explicit asymptotic expansion for the mean FHT (MFHT). For fractional order $s \in (0,1)$ (describing a (2s)-stable Lévy flight whose squared displacement scales as $t^{1/s}$ in time t) and targets of radius $\varepsilon \ll 1$, we show that the MFHT is order one for $s \in (1/2,1)$ and diverges as $\log(1/\varepsilon)$ for s = 1/2 and ε^{2s-1} for $s \in (0,1/2)$. We then use our asymptotic results to identify the value of $s \in (0,1]$ which minimizes the average MFHT and find that (a) this optimal value of s vanishes for sparse targets and (b) the value s = 1/2 (corresponding to an inverse square Lévy search) is optimal in only very specific circumstances. We confirm our results by comparison to both deterministic numerical solutions of the associated fractional differential equation and stochastic simulations.

Key words. anomalous diffusion, first hitting times, asymptotic analysis, fractional differential equation, Lévy flight

MSC codes. 60J60, 35R11, 35C20, 92C40

DOI. 10.1137/23M1586239

1. Introduction. The timescales of many physical, chemical, and biological processes are characterized by first hitting times (FHTs) [4, 57, 17, 56]. Generically, the FHT is the time it takes a "searcher" to find a "target." Applications include animal foraging [62, 31], transcription factor search for DNA binding sites [39, 43], synaptic transmission in neuroscience [58], menopause timing [34], financial income dynamics [27], and computer search algorithms [53, 54], among many other applications [4, 57, 17]. FHTs are often called first passage times, first arrival times, exit times, escape times, or capture times.

Mathematical models of such processes often assume that the searcher randomly explores a given spatial domain, and a great deal of mathematical and computational methods have been developed to study the statistics and probability distribution of the FHT to the target(s) [3, 25, 61, 37, 8, 28]. More precisely, let $X = \{X(t)\}_{t\geq 0}$ denote the stochastic path of a searcher in a d-dimensional spatial domain $\Omega \subseteq \mathbb{R}^d$. The FHT to a target set $\Omega_{\text{target}} \subset \Omega$ (where Ω_{target} is possibly a union of multiple disjoint sets) is then

(1.1)
$$\tau := \inf\{t > 0 : X(t) \in \Omega_{\text{target}}\}.$$

^{*}Received by the editors July 12, 2023; accepted for publication (in revised form) February 28, 2024; published electronically May 29, 2024.

 $[\]rm https://doi.org/10.1137/23M1586239$

Funding: The first author was supported by the Simons Foundation Math + X grant. The second author was supported by the National Science Foundation (DMS-1944574 and DMS-1814832).

[†]Center for Mathematical Biology and Department of Mathematics, University of Pennsylvania, Philadelphia, PA 19104 USA (d1gomez@sas.upenn.edu).

[‡]Department of Mathematics, University of Utah, Salt Lake City, UT 84112 USA (lawley@math.utah.edu).

Naturally, the statistics and distribution of the FHT τ depend on the stochastic dynamics of the searcher X, the space dimension $d \ge 1$, and the size and geometry of the target set Ω_{target} and spatial domain Ω .

A common framework for studying FHTs is to assume that the searcher X is a pure diffusion process (i.e., a Brownian motion) and the targets are much smaller than their confining spatial domain, which is called the narrow capture problem (or narrow escape problem if the target is embedded in the otherwise reflecting boundary) [55, 16, 2, 25, 23, 9]. For bounded domains in dimension d = 1, the MFHT of such a diffusive searcher is always finite even if the targets are single points. In contrast, the MFHT of diffusion in any dimension $d \ge 2$ diverges as the target size vanishes. In particular, if $\varepsilon > 0$ compares the lengthscale of the target to the lengthscale of the confining domain, then it is well known that as ε vanishes,

(1.2)
$$\mathbb{E}[\tau] = \begin{cases} O(1) & \text{if } d = 1, \\ O(\log(1/\varepsilon)) & \text{if } d = 2, \\ O(\varepsilon^{2-d}) & \text{if } d \ge 3. \end{cases}$$

The stark contrast in (1.2) between dimensions d = 1, d = 2, and $d \ge 3$ stems from the fact that Brownian motion is recurrent if d = 1, neighborhood recurrent in d = 2, and transient in $d \ge 3$ [20].

FHTs have also been studied for superdiffusive processes, which are characterized by squared displacements that grow superlinearly in time [42, 15, 40, 50, 32, 49, 46, 45, 65, 24, 14, 47, 60]. A common mathematical model of superdiffusion is a Lévy flight [5, 19], which is often derived from the continuous time random walk model [44, 42]. In this model, a searcher waits at its current location for a random time and then jumps a random distance chosen from some jump length probability density f(y) in a uniform random direction. The searcher repeats these two steps indefinitely or until it reaches the target. For a finite mean waiting time $t_0 \in (0, \infty)$ and a jump length density with the following slow power law decay,

(1.3)
$$f(y) \sim \frac{(l_0)^{2s}}{y^{1+2s}}$$
 as $y \to \infty$ for some $s \in (0,1)$ and lengthscale $l_0 > 0$,

the probability density p(x,t) for the searcher position satisfies the following space-fractional Fokker-Planck equation in a certain scaling limit [41],

(1.4)
$$\frac{\partial}{\partial t}p = -D_s(-\Delta)^s p,$$

where $(-\Delta)^s$ denotes the fractional Laplacian of order $s \in (0,1)$, defined by [38]

(1.5)
$$(-\Delta)^{s} \varphi(x) = C_{s} \text{P.V.} \int_{-\infty}^{\infty} \frac{\varphi(x) - \varphi(y)}{|x - y|^{2s + d}} dy, \qquad C_{s} := \frac{4^{s} \Gamma(s + d/2)}{\pi^{d/2} |\Gamma(-s)|},$$

where P.V. indicates the principal value and $\Gamma(\cdot)$ denotes the gamma function. In (1.4), the parameter D_s is the s-dependent generalized diffusivity and is given by

$$(1.6) D_s = (l_0)^{2s}/t_0 > 0,$$

where l_0 and t_0 are characteristic spatial and temporal scales of the Lévy flight. Note that fixing l_0 and t_0 allows us to compare search strategies as the fractional order is varied. This will be particularly important when we address the optimality of

Lévy flights in section 4. Note also that Lévy flights are often parameterized by their stability index $\alpha \in (0, 2)$ [48], which is simply twice the fractional order $s \in (0, 1)$,

$$\alpha = 2s \in (0, 2).$$

Observe that (1.4) is the diffusion equation describing Brownian motion if s=1.

Lévy flights are perhaps the most mathematically tractable model of superdiffusion, though analytical results for Lévy flights are scarce compared to their Brownian counterpart. The mathematical analysis of hitting times of superdiffusive search processes has also been controversial. Indeed, the influential Lévy flight foraging hypothesis was based on the claimed theoretical optimality of a certain superdiffusive process involving heavy-tailed jumps as in (1.3) with the "inverse square" value s = 1/2 [63, 62], but this decades-old claim was recently shown to be false [35, 11, 36].

In this paper, we study FHTs of Lévy flights to small targets in one space dimension. Assuming the targets are much smaller than the typical distance between them, we apply the method of matched asymptotic expansions to the fractional differential equation describing the MFHT. The resulting asymptotic formulas reveal how FHTs depend on the fractional order $s \in (0,1)$, target size, target arrangement, and initial searcher location (or distribution of locations). We further determine the full probability distribution of the FHT for fractional orders $s \in (0,1/2]$ in the small target limit. We validate our results by comparison to both deterministic numerical solutions of the associated fractional differential equation and stochastic simulations.

To describe our results more precisely, let $X = \{X(t)\}_{t\geq 0}$ be a one-dimensional, (2s)-stable Lévy flight for $s \in (0,1)$ with generalized diffusivity $D_s > 0$ (i.e., the probability density that X(t) = x satisfies (1.4)) and periodic boundary conditions at $x = \pm l$. Since we can always rescale space and time according to

$$(1.7) x \to x/l, \quad t \to D_s t/l^{2s},$$

we set $D_s = l = 1$ without loss of generality. Suppose that the target set Ω_{target} consists of $N \geq 1$ targets in the interval $\Omega = (-1,1) \in \mathbb{R}$ centered at points $\{x_1, \ldots, x_N\} \in (-1,1)$ with radii $\{\varepsilon l_1, \ldots, \varepsilon l_N\}$, i.e.,

(1.8)
$$\Omega_{\text{target}} = \bigcup_{i=1}^{N} (x_i - \varepsilon l_i, x_i + \varepsilon l_i).$$

Here, $l_1, \ldots, l_N > 0$ are O(1) constants which allow the targets to differ in size. When the context is clear, we denote by $|\cdot|$ the 2-periodic extension of the absolute value on (-1,1) so that |a-b| denotes the minimum distance between a and b in the periodic domain (-1,1). Assume that $0 < \varepsilon \ll 1$ and the targets are well-separated in the sense that $|x_i - x_j| \gg \varepsilon$ for all $i, j \in \{1, \ldots, N\}$ with $i \neq j$. Let v(x) denote the MFHT to any of the N targets starting from $x \in (-1,1)$, i.e.,

$$v(x) := \mathbb{E}[\tau \mid X(0) = x],$$

where τ is the FHT in (1.1). The function v(x) satisfies (see Appendix B)

(1.9)
$$\begin{cases} (-\Delta)^s v(x) = 1, & x \in \Omega \setminus \Omega_{\text{target}}, \\ v(x) = 0, & x \in \Omega_{\text{target}}, \\ v(x) \text{ is 2-periodic.} \end{cases}$$

We obtain our results on the FHT by analyzing (1.9) in the limit $\varepsilon \to 0$.

We now state our results on the MFHT for the case of a single target of radius $\varepsilon > 0$ centered at $x_1 = 0$ (i.e., $N = l_1 = 1$). Note that our assumption of periodic boundary conditions means that this scenario is equivalent to a Lévy flight on all of \mathbb{R} with a periodic array of targets separated by distance 2. For any fractional order $s \neq 1/2$, the MFHT of a Lévy flight conditioned on starting at $x \in (-1,1) \setminus \{0\}$ is given by the following asymptotic formula for $0 < \varepsilon \ll 1$,

$$(1.10) v(x) \sim \varepsilon^{2s-1} \frac{2\mathfrak{a}_s}{\mathfrak{b}_s} - 2\mathfrak{a}_s R_s(0) + 2\mathfrak{a}_s \left(-|x|^{2s-1} + R_s(x)\right),$$

where

(1.11)
$$\mathfrak{a}_s := -2\pi^{-1} s \Gamma(-2s) \sin(\pi s), \quad \mathfrak{b}_s := \frac{\Gamma(1/2)}{\Gamma(3/2 - s) \Gamma(s)},$$

and R_s is the regular part of the Green's function given explicitly in Proposition 2.2. If s = 1/2, then this MFHT is

(1.12)
$$v(x) \sim \log(2/\varepsilon) \frac{2}{\pi} - \frac{2}{\pi} R_{1/2}(0) + \frac{2}{\pi} (\log|x| + R_{1/2}(x)).$$

If the Lévy flight searcher starts from a uniformly distributed position in the interval (-1,1), then the average MFHT is

(1.13)
$$\frac{1}{2} \int_{-1}^{1} v(x) dx \sim \begin{cases} \varepsilon^{2s-1} 2\mathfrak{a}_{s}/\mathfrak{b}_{s} - R_{s}(0) 2\mathfrak{a}_{s} & \text{if } s \neq 1/2, \\ \log(2/\varepsilon) 2/\pi - 2R_{1/2}(0)/\pi & \text{if } s = 1/2. \end{cases}$$

These results show an analogue between Brownian search in dimensions $d \ge 1$ and Lévy search in dimension d = 1 with fractional order $s \in (0,1)$. Specifically, (1.10)-(1.13) imply

(1.14)
$$\mathbb{E}[\tau] = \begin{cases} O(1) & \text{if } s \in (1/2, 1], \\ O(\log(1/\varepsilon)) & \text{if } s = 1/2, \\ O(\varepsilon^{2s-1}) & \text{if } s \in (0, 1/2). \end{cases}$$

Comparing (1.2) to (1.14) shows that FHTs of Brownian motion in different dimensions diverge similarly to FHTs of Lévy flights in one dimension with different fractional orders. As in the case of Brownian motion in (1.2), the different regimes in (1.14) stem from differences in recurrence versus transience, which manifests in our analysis as different far-field behavior of the inner solutions used in our matched asymptotics. FHTs of Lévy flights in one dimension can diverge because the stochastic paths of Lévy flights are discontinuous. Hence, in contrast to Brownian motion, Lévy flights may jump across a target without actually hitting it in a phenomenon termed a "leapover" [30, 29, 48, 64] (see Figure 1 for an illustration).

Our analysis allows us to identify the value of $s \in (0,1]$ which minimizes the MFHT. We find that this optimal value (denoted by $s_{\rm opt}$) grows continuously from $s_{\rm opt} \approx 0$ up to $s_{\rm opt} \approx 1$ (i.e., Brownian search) as the target density grows relative to the lengthscale l_0 in (1.3)–(1.6). In particular, we show that the value s = 1/2 (corresponding to stability index $\alpha = 2s = 1$, i.e., inverse square Lévy search) is optimal in only very specific circumstances.

The rest of the paper is organized as follows. In section 2, we analyze the mean and full probability distribution of the FHT. In section 3, we compare our asymptotic

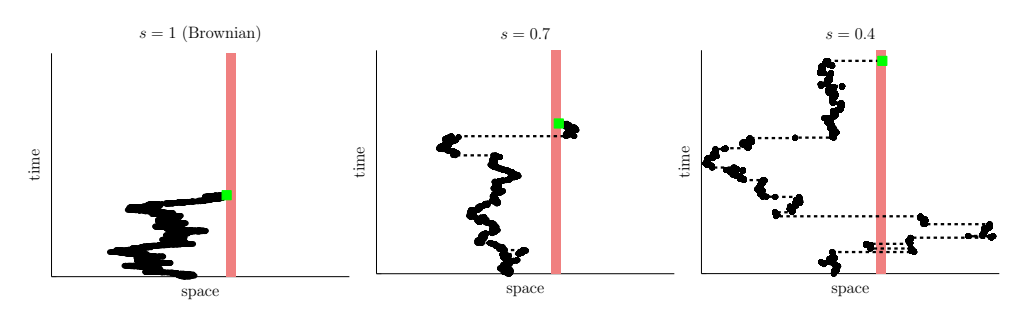


Fig. 1. Lévy flight sample paths in one space dimension for (left) s=1 (i.e., Brownian motion), (middle) s=0.7, and (right) s=0.4. The solid black markers show positions of the Lévy flight. For s<1, the black dashed lines show the discontinuous jumps of the Lévy flight, which become larger for smaller values of $s \in (0,1)$ and allow the Lévy flight to jump across the target (regions with red vertical lines).

results to numerical solutions of the associated fractional equations and stochastic simulations. In section 4, we address the question of the fractional order $s \in (0,1]$ that minimizes the MFHT. We conclude by summarizing our results and discussing related work. Appendix A collects some more technical aspects of the numerical implementation in section 3, while Appendix B includes a derivation of the fractional equations for the FHT moments.

2. Asymptotic analysis of the MFHT. The method of matched asymptotic expansions (MMAE) has been an invaluable tool in the analysis of narrow capture and escape problems for pure diffusion processes since its introduction in [55, 16]. Broadly speaking, the MMAE proceeds by formulating inner- and outer-problems whose solutions can be expressed in terms of a canonical "electrified disk" solution and an appropriately weighted sum of Green's functions, respectively. Combining a solvability condition for the outer-problem together with matching conditions between the inner- and outer-solutions yields a linear system with which all remaining unknowns arising in the asymptotic analysis can be determined. In this section, we adapt the MMAE to derive an asymptotic expansion for the MFHT satisfying the fractional differential equation (1.9). We show how the MMAE in this fractional setting synthesizes the analysis of the standard narrow escape problem in dimensions d=2 and d=3. In addition, we introduce a fractional counterpart to the classical electrified disk problem, as well as a 2-periodic fractional Green's function.

We begin our asymptotic analysis of the MFHT by seeking an outer asymptotic expansion of the form

$$(2.1a) v(x) \sim v_0^{\varepsilon}(x),$$

valid for values of x that are sufficiently far from all targets in the sense that $|x-x_i|\gg \varepsilon$ for all $i=1,\ldots,N$. In addition, for each $i=1,\ldots,N$ we seek an inner asymptotic expansion of the form

(2.1b)
$$v(x_i + \varepsilon X) \sim V_i^{\varepsilon}(X),$$

valid for values of $x = x_i + \varepsilon X$ sufficiently close to the *i*th target in the sense that X = O(1). Note that in (2.1) and throughout the remainder of the paper, we use a superscript ε to denote a general dependence on this parameter.

It is here convenient to recall two equivalent definitions of the fractional Laplacian given by (1.5) when restricted to 2-periodic functions. Specifically, if we let $\varphi(x)$ be an arbitrary 2-periodic function, then

(2.2a)
$$(-\Delta)^s \varphi(x) = C_s \text{P.V.} \int_{-1}^1 K_s(x - y)(\varphi(x) - \varphi(y)) dy,$$

where

(2.2b)
$$K_s(z) := \sum_{n \in \mathbb{Z}} \frac{1}{|z + 2n|^{2s+1}}$$

and where \mathbb{Z} denotes the set of all integers. This expression is conveniently chosen to determine appropriate inner problems. Moreover, it can be shown (see, for example, equation (2.53) in [1]) that the restriction of the fractional Laplacian defined by (1.5) to 2-periodic functions coincides with the spectral fractional Laplacian defined by

$$(2.3) \qquad (-\Delta)^s \varphi(x) = \sum_{n=\mathbb{Z}\setminus\{0\}} |n\pi|^{2s} \varphi_n e^{in\pi x}, \qquad \varphi_n := \frac{1}{2} \int_{-1}^1 e^{-in\pi x} \varphi(x) dx.$$

This formulation proves to be useful when considering global quantities, such as the relevant periodic fractional Green's function.

In order to state our main result for this section, we first define the scalars

(2.4a)
$$\nu_i^{\varepsilon} := -\frac{1}{\log(\varepsilon l_i/2)}, \qquad \bar{\nu}^{\varepsilon} := \frac{1}{N} \sum_{i=1}^N \nu_i^{\varepsilon}, \qquad \bar{l}_s := \frac{1}{N} \sum_{i=1}^N l_i^{1-2s},$$

as well as the N-dimensional vectors

(2.4b)
$$\boldsymbol{l}_s := \begin{pmatrix} l_1^{1-2s} \\ \vdots \\ l_N^{1-2s} \end{pmatrix}, \quad \boldsymbol{\nu}^{\varepsilon} := \begin{pmatrix} \nu_1^{\varepsilon} \\ \vdots \\ \nu_N^{\varepsilon} \end{pmatrix}, \quad \boldsymbol{e}_N := \begin{pmatrix} 1 \\ \vdots \\ 1 \end{pmatrix}.$$

In addition, we define the $N \times N$ diagonal matrices

(2.4c)
$$\mathcal{L}_s := \operatorname{diag}\left(l_1^{1-2s}, \dots, l_N^{1-2s}\right), \qquad \mathcal{N}^{\varepsilon} := \operatorname{diag}(\nu_1^{\varepsilon}, \dots, \nu_N^{\varepsilon}),$$

as well as the $N \times N$ Green's matrix \mathcal{G}_s whose entries are given by

(2.4d)
$$(\mathcal{G}_s)_{ij} = \begin{cases} R_s(0), & i = j, \\ R_s(x_i - x_j) + H_s(x_i - x_j), & i \neq j, \end{cases}$$

where R_s is the regular part of the Green's function defined in Proposition 2.2, and $H_s(z)$ is the singular part with $H_s(z) := -|z|^{2s-1}$ for $s \neq 1/2$ and $H_s(z) := \log|z|$ for s = 1/2. Our main asymptotic result for the hitting time is given below.

PRINCIPAL RESULT 1. Let $\varepsilon \ll 1$, let $l_1, \ldots, l_N = O(1)$, and suppose that $-1 \le x_1 < \cdots < x_N < 1$ are well-separated in the sense that $|x_i - x_j| \gg O(\varepsilon)$ for all $i \ne j$. For any 0 < s < 1, define

(2.5a)
$$\chi^{\varepsilon} := \begin{cases} \frac{1}{N\bar{l}_s} \left(\frac{2\mathfrak{a}_s}{\mathfrak{b}_s} \varepsilon^{2s-1} - \varepsilon^{1-2s} \mathfrak{b}_s \boldsymbol{l}_s^T \mathcal{G}_s \mathcal{L}_s \boldsymbol{B}^{\varepsilon} \right), & s \neq 1/2, \\ \frac{2}{\pi N \bar{\nu}^{\varepsilon}} \left(1 - \frac{\pi}{2} (\boldsymbol{\nu}^{\varepsilon})^T \mathcal{G} \boldsymbol{B}^{\varepsilon} \right), & s = 1/2, \end{cases}$$

where \mathfrak{a}_s and \mathfrak{b}_s are given by (1.11) and where the N-dimensional vector $\mathbf{B}^{\varepsilon} = (B_1^{\varepsilon}, \dots, B_N^{\varepsilon})^T$ is found by solving the linear system

(2.5b)
$$\begin{cases} \left(\mathcal{I}_{N} - \varepsilon^{1-2s} \mathfrak{b}_{s} \left(\mathcal{I}_{N} - \frac{1}{N \bar{l}_{s}} \boldsymbol{e}_{N} \boldsymbol{l}_{s}^{T} \right) \mathcal{G}_{s} \mathcal{L}_{s} \right) \boldsymbol{B}^{\varepsilon} = \frac{2\mathfrak{a}_{s} \varepsilon^{2s-1}}{N \bar{l}_{s} \mathfrak{b}_{s}} \boldsymbol{e}_{N}, & s \neq 1/2, \\ \left(\mathcal{I}_{N} - \mathcal{N}^{\varepsilon} \left(\mathcal{I}_{N} - \frac{1}{N \bar{\nu}^{\varepsilon}} \boldsymbol{e}_{N} (\boldsymbol{\nu}^{\varepsilon})^{T} \right) \mathcal{G}_{1/2} \right) \boldsymbol{B}^{\varepsilon} = \frac{2}{\pi N \bar{\nu}^{\varepsilon}} \boldsymbol{\nu}^{\varepsilon}, & s = 1/2, \end{cases}$$

where \mathcal{I}_N is the $N \times N$ identity matrix. Then, an asymptotic expression for the MFHT satisfying (1.9) for $|x - x_i| \gg \varepsilon$ for all i = 1, ..., N is given by

$$(2.5c) v(x) \sim \chi^{\varepsilon} + \begin{cases} \mathfrak{b}_{s} \varepsilon^{1-2s} \sum_{j=1}^{N} l_{j}^{1-2s} B_{j}^{\varepsilon} (-|x-x_{j}|^{2s-1} + R_{s}(x-x_{j})), & s \neq 1/2, \\ \sum_{j=1}^{N} B_{j}^{\varepsilon} \left(\log|x-x_{j}| + R_{1/2}(x-x_{j}) \right), & s = 1/2, \end{cases}$$

where $R_s(x)$ is the regular part of the Green's function found in Proposition 2.2.

The remainder of this section is organized as follows. In sections 2.1 and 2.2, we first establish key properties of two quantities relevant to the construction of inner and outer solutions, respectively. Specifically, in section 2.1 we consider a fractional counterpart to the classical electrified disk problem. This is followed by a discussion of a certain 2-periodic fractional Green's function in section 2.2. In section 2.3, we then proceed with applying the MMAE to derive Principal Result 1. Finally, in section 2.4 we show that, to leading order, the FHT τ is exponentially distributed for $s \in (0, 1/2]$.

2.1. The fractional electrified disk problem. Substituting the change of variables $X = (x - x_i)/\varepsilon$ into (1.9), we obtain a leading order homogeneous problem for the inner solution $V_i^{\varepsilon}(X)$ (see section 2.3 below). The scaling invariance of this problem suggests that $V_i^{\varepsilon}(X)$ is proportional to the solution of some canonical problem, where the constant of proportionality acts as a degree of freedom with which to match inner and outer solutions. A natural choice for the corresponding canonical problem is the fractional counterpart to the electrified disk problem, which is given by

(2.6)
$$\begin{cases} (-\Delta)^s W_s(X) = 0, & |X| > 1, \\ W_s(X) = 1, & |X| < 1, \end{cases}$$

and for which we now collect several key properties. The function $W_s(X)$ is the probability that a Lévy flight starting at $X \in \mathbb{R}$ eventually hits the ball (-1,1). With this probabilistic interpretation, one readily obtains the following formula for $W_s(X)$ when s < 1/2 (see Corollary 2 in [7]):

$$(2.7) \hspace{1cm} W_s(X) = \frac{\sqrt{\pi}}{\Gamma\left(\frac{1}{2}-s\right)\Gamma(s)} \int_{X^2-1}^{\infty} \frac{u^{s-1}}{\sqrt{u+1}} du.$$

We proceed to derive an explicit expression for $W_s(X)$ valid for all $s \in (0,1)$. Specifically, we deploy a Kelvin transform and fractional Poisson formula for $s \neq 1/2$ and standard complex analysis tools for s = 1/2. The main result is summarized in the following proposition.

Proposition 2.1. The fractional electrified disk problem (2.6) admits the following nonconstant solution:

(2.8a) $W_s(X)$

$$= \begin{cases} \frac{\sqrt{\pi}}{\Gamma(s)\Gamma\left(\frac{3}{2}-s\right)}|X|^{2s-1}\left(1-\frac{1}{X^2}\right)^s {}_2F_1\left(1,\frac{1}{2};\frac{3}{2}-s;\frac{1}{X^2}\right), & s\neq 1/2, \\ 1-\log(X+\sqrt{X^2-1}), & s=1/2, \end{cases} |X|>1,$$

with $W_s(X) = 1$ for $|X| \le 1$. Moreover, this solution has the far-field behavior

(2.8b)
$$W_s(X) \sim \begin{cases} \mathfrak{b}_s |X|^{2s-1} + O(|X|^{2s-3}), & s \neq 1/2, \\ -\log(2|X|) + 1 + O(X^{-2}), & s = 1/2, \end{cases} \quad as \quad |X| \to \infty,$$

where \mathfrak{b}_s is given by (1.11).

Starting with the $s \neq 1/2$ case, we first transform (2.6) into the more commonly considered fractional problem with extended Dirichlet boundary conditions posed outside of (-1,1). Specifically, we first use the Kelvin transform

(2.9a)
$$\overline{X} = 1/X, \quad \overline{W}_s(\overline{X}) = |\overline{X}|^{2s-1}W_s(1/\overline{X}),$$

in terms of which we readily calculate (see, for example, Proposition A.1 in [59])

$$(2.9b) \qquad (-\Delta)^s \overline{W}_s(\overline{X}) = |X|^{2s+1} (-\Delta)^s W_s(X).$$

In particular, we find that $\overline{W}_s(\overline{X})$ solves

(2.10)
$$\begin{cases} (-\Delta)^s \overline{W}_s(\overline{X}) = 0, & |\overline{X}| < 1, \\ \overline{W}_s(\overline{X}) = |\overline{X}|^{2s-1}, & |\overline{X}| > 1. \end{cases}$$

Notice that the inhomogeneous term $g(\overline{X}) = |\overline{X}|^{2s-1}$ for $|\overline{X}| > 1$ in (2.10) can be extended to $\mathbb R$ in such a way that $g \in L^1_{\mathrm{loc}}(\mathbb R) \cap C(\mathbb R)$ and

$$\int_{\mathbb{R}} \frac{|g(\overline{X})|}{1 + |\overline{X}|^{1+2s}} d\overline{X} < \infty.$$

It then follows that the unique *continuous* solution to (2.10) is given by (see Theorem 2.10 in [10])

$$\overline{W}_s(\overline{X}) = \begin{cases} \int_{|Y| > 1} P_s(Y, \overline{X}) |Y|^{2s - 1} dY, & |\overline{X}| < 1, \\ |\overline{X}|^{2s - 1}, & |\overline{X}| > 1, \end{cases}$$

where $P_s(y,x)$ is the fractional Poisson kernel given by

$$P_s(y,x) := p_s \left(\frac{1-x^2}{y^2-1}\right)^s \frac{1}{|x-y|}, \qquad p_s := \pi^{-1} \sin(\pi s) = \frac{1}{\Gamma(s)\Gamma(1-s)}.$$

Reverting to the original variables, we therefore obtain the integral representation

$$\begin{split} W_s(X) &= p_s \int_1^\infty \left(\frac{X^2 - 1}{1 - 1/Y^2}\right)^s \frac{2|X|}{(XY)^2 - 1} dY \\ &= p_s |X|^{2s - 1} \left(1 - \frac{1}{X^2}\right)^s \int_0^\infty \frac{(z + 1)^{s - \frac{1}{2}}}{z^s \left(z + 1 - \frac{1}{X^2}\right)} dz, \end{split}$$

where the first equality follows by combining the $Y \in (-\infty, -1)$ and $Y \in (1, \infty)$ contributions and the second from the change of variables $Y = \sqrt{z+1}$. Using the integral representation of the Gaussian hypergeometric function (see equation 15.6.1 in [18]), we immediately obtain (2.8a). The far-field behavior (2.8b) of $W_s(X)$ is likewise immediately obtained by noting that (see equation 15.2.1 in [18])

$${}_2F_1\left(1,\frac{1}{2};\frac{3}{2}-s;z\right) = 1 + \frac{z}{3-2s} + \frac{3z^2}{4s^2-16s+15} + O(z^3), \qquad |z| \ll 1.$$

Remark 2.1. The equivalence of (2.8a) and (2.7) is readily verified using properties of the Gaussian hypergeometric function. Specifically, we first recast the integral in (2.7) in terms of the Gaussian hypergeometric function using the change of variables $u = X^2(z+1) - 1$. Equivalence with (2.8a) is then verified by first using Euler's transformation ${}_2F_1(a,b;c;z) = (1-z)^{c-a-b}{}_2F_1(c-a,c-b;c;z)$ and then using the symmetry property ${}_2F_1(a,b;c;z) = {}_2F_1(b,a;c;z)$.

We consider next the case s=1/2 for which the previous calculations yield $W_s(X) \equiv 1$. Indeed, it is easy to see that $\overline{W}_s(\overline{X}) \equiv 1$ is the unique continuous solution to (2.10) when s=1/2. To find a nonconstant solution to (2.6), we instead consider the extended problem in the two-dimensional upper half-space. Specifically, we seek a nonconstant solution $\widetilde{W}(X,Y)$ to

$$\begin{cases} \frac{\partial^2 \widetilde{W}}{\partial X^2} + \frac{\partial^2 \widetilde{W}}{\partial Y^2} = 0, & -\infty < X < \infty, Y > 0, \\ \widetilde{W} = 1, & |X| < 1, Y = 0, \\ \frac{\partial \widetilde{W}}{\partial Y} = 0, & |X| > 1, Y = 0, \end{cases}$$

in terms of which $W_{s=1/2}(X) = \widetilde{W}(X,0)$ (see [12] for additional details on the extension property of the fractional Laplacian). Such a nonconstant solution must have logarithmic growth as $X^2 + Y^2 \to \infty$ and is given by

$$\widetilde{W}(X,Y) = 1 + \operatorname{Im}\{\arcsin(X+iY)\},$$

where Im(z) denotes the imaginary part of $z \in \mathbb{C}$. Setting Y = 0 and considering only values of |X| > 1, we readily obtain (2.8a) from which the far-field behavior (2.8b) immediately follows.

2.2. The periodic fractional Green's function. Asymptotic matching prescribes the limiting behavior of the outer solution as $x \to x_i$ for each i = 1, ..., N (see section 2.3 below). The resulting limiting behavior in turn implies that the outer solution can be written as a weighted sum of translations of a fractional Green's function $G_s(x)$ satisfying

(2.12)
$$\begin{cases} (-\Delta)^s G_s(x) = \frac{1}{2} - \delta(x), & -1 < x < 1, \\ G_s(x+2) = G(x), & -\infty < x < \infty, \\ \int_{-1}^1 G_s(x) dx = 0. \end{cases}$$

Using the spectral definition of the fractional Laplacian (2.3), it is straightforward to see that

(2.13)
$$G_s(x) = -\sum_{n=1}^{\infty} \frac{\cos n\pi x}{(n\pi)^{2s}}.$$

We readily see that $G_s(x)$ diverges as $x \to 0$ for $s \le 1/2$. The following proposition extracts this singular behavior and decomposes $G_s(x)$ into a *singular* part and a *regular* part.

PROPOSITION 2.2. The periodic fractional Green's function $G_s(x)$ satisfying (2.12) is given by

(2.14a)
$$G_s(x) = \begin{cases} -\mathfrak{a}_s |x|^{2s-1} + \mathfrak{a}_s R_s(x), & s \neq 1/2, \\ \pi^{-1} \log |x| + \pi^{-1} R_{1/2}(x), & s = 1/2, \end{cases}$$

where \mathfrak{a}_s is given by (1.11). When $s \neq 1/2$, the regular part $R_s(x)$ admits the following rapidly converging series,

$$(2.14b)$$

$$R_s(x) = \frac{1}{2s} - \frac{2s-1}{6} + \frac{7}{15} \frac{(2s-1)(2s-2)(2s-3)}{24} + \left(\frac{2s-1}{2} - \frac{(2s-1)(2s-2)(2s-3)}{12}\right) |x|^2 + \frac{(2s-1)(2s-2)(2s-3)}{24} |x|^4 + 2(2s-1)\cdots(2s-5) \sum_{n=1}^{\infty} \frac{a_{2s,n}}{(\pi n)^{2s}} \cos(\pi n x),$$

where $a_{2s,n} = \int_{\pi n}^{\infty} x^{2s-6} \sin x dx$. On the other hand, when s = 1/2, the regular part has the series expansion

(2.14c)
$$R_{1/2}(x) = 1 + 2\sum_{n=1}^{\infty} \left(\text{Si}(n\pi) - \frac{\pi}{2} \right) \frac{\cos n\pi x}{n\pi},$$

where $\operatorname{Si}(z) = \int_0^z t^{-1} \sin(t) dt$ denotes the usual sine integral.

The calculation of $G_s(x)$ in the case $s \neq 1/2$ follows from computing Fourier series of $|x|^2$, $|x|^4$, and $|x|^{2s-1}$ and can be found in Appendix A of [22]. The case s = 1/2 follows similarly, but this time only the Fourier series of $\log |x|$ is needed.

For the subsequent asymptotic analysis, the most important part of $G_s(x)$ in (2.14a) is the *singular* behavior which takes the form of an algebraic singularity for s < 1/2, a logarithmic singularity for s = 1/2, and a bounded fractional cusp for s > 1/2. The series expansions for the regular part appearing in (2.14b) and (2.14c), on the other hand, are computationally useful due to their fast convergence.

2.3. Matched asymptotic expansions. Let $x = x_i + \varepsilon X$, and substitute the inner expansion (2.1b) into (1.9) so that using (2.2) for the fractional Laplacian we obtain

(2.15)
$$\varepsilon C_s \text{P.V.} \int_{-1/\varepsilon}^{1/\varepsilon} \sum_{n \in \mathbb{Z}} \frac{V_i^{\varepsilon}(X) - V_i^{\varepsilon}(Y)}{|2n + \varepsilon(X - Y)|^{2s+1}} dY + \text{h.o.t.} = 1,$$

where h.o.t. denotes higher-order terms. The n=0 term dominates all other terms in the left-hand side, and moreover we will also assume that it dominates the right-hand side by assuming that $V_i^{\varepsilon} \gg \varepsilon^{2s}$ for all X = O(1). Further approximating the integral on the left-hand side by replacing $\pm 1/\varepsilon$ with $\pm \infty$, we thus obtain the inner problem

(2.16)
$$\begin{cases} (-\Delta)^s V_i^{\varepsilon}(X) = 0, & |X| > l_i, \\ V_i^{\varepsilon}(X) = 0, & |X| \le l_i, \end{cases}$$

where the limiting behavior of $V_i^{\varepsilon}(X)$ as $|X| \to \infty$ will be found by matching with the limiting behavior of the outer solution as $x \to x_i$ for each i = 1, ..., N.

In light of Proposition 2.1, we seek, for each i = 1, ..., N, a nonconstant inner solution of the form

$$(2.17) V_i^{\varepsilon}(X) = B_i^{\varepsilon} \left(1 - W_s(X/l_i)\right),$$

where B_i^{ε} is some ε -dependent constant that remains to be determined. From Proposition 2.1 we then have the far-field behavior

$$V_i^{\varepsilon}(X) \sim \begin{cases} B_i^{\varepsilon} \left(1 - \mathfrak{b}_s l_i^{1-2s} |X|^{2s-1} + O(|X|^{2s-3}) \right), & s \neq 1/2, \\ B_i^{\varepsilon} \left(\log(2|X/l_i|) + O(|X|^{-2}) \right), & s = 1/2, \end{cases} \text{ as } |X| \to \infty.$$

The far-field behavior of $V_i^{\varepsilon}(X)$ must coincide with the limiting behavior of the outer solution $v_0^{\varepsilon}(x)$ as $x \to x_i$. Specifically, writing $X = \varepsilon^{-1}(x - x_i)$ we obtain the matching condition as $|x - x_i| \to 0$,

$$(2.18) \hspace{1cm} v_0^\varepsilon(x) \sim \begin{cases} B_i^\varepsilon \left(1 - \mathfrak{b}_s \varepsilon^{1-2s} l_i^{1-2s} |x-x_i|^{2s-1} + O(\varepsilon^{3-2s})\right), & s \neq 1/2, \\ B_i^\varepsilon \left(\log |x-x_i| + 1/\nu_i^\varepsilon + O(\varepsilon^2)\right), & s = 1/2. \end{cases}$$

Given the singular term $|x-x_i|^{2s-1}$ in the limiting behavior (2.18), we find that $v_0^{\varepsilon}(x)$ is the 2-periodic function satisfying

$$(2.19) \qquad (-\Delta)^{s} v_{0}^{\varepsilon}(x) = \begin{cases} 1 - \varepsilon^{1-2s} \mathfrak{a}_{s}^{-1} \mathfrak{b}_{s} \sum_{j=1}^{N} l_{j}^{1-2s} B_{j}^{\varepsilon} \delta(x - x_{j}), & s \neq 1/2, \\ 1 - \pi \sum_{j=1}^{N} B_{j}^{\varepsilon} \delta(x - x_{j}), & s = 1/2. \end{cases}$$

Since this problem is posed on the whole (periodic) interval -1 < x < 1, we can now use the spectral definition (2.3) for the fractional Laplacian so that by integrating (2.19) over the domain we obtain the solvability conditions

(2.20)
$$\mathfrak{a}_{s}^{-1}\mathfrak{b}_{s}\sum_{j=1}^{N}l_{j}^{1-2s}B_{j}^{\varepsilon}=2\varepsilon^{2s-1}, \qquad \sum_{j=1}^{N}B_{j}^{\varepsilon}=\frac{2}{\pi},$$

for $s \neq 1/2$ and s = 1/2, respectively. Provided this condition is satisfied, we can then write $v_0^{\varepsilon}(x)$ in terms of the periodic fractional Green's function found in Proposition 2.2 as

$$(2.21) \quad v_0^{\varepsilon}(x) = \chi^{\varepsilon} + \begin{cases} \varepsilon^{1-2s} \mathfrak{b}_s \sum_{j=1}^{N} l_j^{1-2s} B_j^{\varepsilon} (-|x-x_j|^{2s-1} + R_s(x-x_j)), & s \neq 1/2, \\ \sum_{j=1}^{N} B_j^{\varepsilon} \left(\log|x-x_j| + R_{1/2}(x-x_j) \right), & s = 1/2, \end{cases}$$

where χ^{ε} is an undetermined constant.

The asymptotic analysis has thus far yielded an expression for the outer solution in terms of the N+1 unknown quantities $B_1^{\varepsilon}, \ldots, B_N^{\varepsilon}$ and χ^{ε} . The solvability condition (2.20) yields one equation in these N+1 unknowns. By revisiting the matching condition (2.18) we obtain the remaining N equations with which all N+1 unknowns

can be uniquely determined. Specifically, substituting the asymptotic expansion of (2.21) as $x \to x_i$ into the left-hand side of (2.18) gives the matching condition

$$\varepsilon^{1-2s}\mathfrak{b}_s l_i^{1-2s} B_i^\varepsilon R_s(0) + \varepsilon^{1-2s}\mathfrak{b}_s \sum_{j \neq i} l_j^{1-2s} B_j^\varepsilon (-|x_i-x_j|^{2s-1} + R_s(x_i-x_j)) + \chi^\varepsilon = B_i^\varepsilon$$

when $s \neq 1/2$ and

$$B_i^{\varepsilon} R_{1/2}(0) + \sum_{j \neq i} B_j^{\varepsilon} \left(\log|x_i - x_j| + R_{1/2}(x_i - x_j) \right) + \chi^{\varepsilon} = B_i^{\varepsilon} / \nu_i^{\varepsilon}$$

when s = 1/2 for each i = 1, ..., N. In light of the definitions (2.4), we can rewrite the solvability and matching conditions in vector notation as

$$\begin{cases} \boldsymbol{l}_s^T \boldsymbol{B}^\varepsilon = \frac{2\mathfrak{a}_s}{\mathfrak{b}_s} \varepsilon^{2s-1}, & \boldsymbol{B}^\varepsilon - \varepsilon^{1-2s} \mathfrak{b}_s \mathcal{G}_s \mathcal{L}_s \boldsymbol{B}^\varepsilon = \chi^\varepsilon \boldsymbol{e}_N, & s \neq 1/2, \\ \boldsymbol{e}_N^T \boldsymbol{B}^\varepsilon = \frac{2}{\pi}, & \boldsymbol{B}^\varepsilon - \mathcal{N}^\varepsilon \mathcal{G}_{1/2} \boldsymbol{B}^\varepsilon = \chi^\varepsilon \boldsymbol{\nu}^\varepsilon, & s = 1/2. \end{cases}$$

Left-multiplying the matching condition in the $s \neq 1/2$ (respectively, s = 1/2) case by \boldsymbol{l}_s^T (respectively, \boldsymbol{e}_N^T) and using the solvability condition yields the expression for χ^{ε} found in (2.5a). Substituting this expression for χ^{ε} back into the matching condition then gives the linear system (2.5b).

We claim that the solution \mathbf{B}^{ε} to (2.5b) is $O(\varepsilon^{2s-1})$ for all $s \in (0,1)$. Indeed, when s < 1/2 we readily obtain the expansion

$$oldsymbol{B}^arepsilon = rac{2\mathfrak{a}_sarepsilon^{2s-1}}{Nar{l}_s\mathfrak{b}_s}\sum_{q=0}^\inftyarepsilonarepsilon^{q(1-2s)}\mathcal{J}_s^qoldsymbol{e}_N, \qquad \mathcal{J}_s := \mathfrak{b}_s\left(\mathcal{I}_N - rac{1}{Nar{l}_s}oldsymbol{e}_Noldsymbol{t}_s^T
ight)\mathcal{G}_s\mathcal{L}_s.$$

Similarly, when s=1/2 we obtain an expansion in powers of $\nu_1^{\varepsilon}, \dots, \nu_N^{\varepsilon}$ starting with an O(1) term since $\boldsymbol{\nu}^{\varepsilon}/\bar{\nu}^{\varepsilon} = O(1)$. When s>1/2, we must proceed by imposing a solvability condition. Specifically, assuming that \mathcal{G}_s is invertible we find that the kernel of \mathcal{J}_s is one-dimensional and spanned by $\boldsymbol{\xi}_s = \mathcal{L}_s^{-1} \mathcal{G}_s^{-1} \boldsymbol{e}_N$. Seeking an expansion of the form $\boldsymbol{B}^{\varepsilon} = \varepsilon^{2s-1} \boldsymbol{B}_0 + \varepsilon^{2(2s-1)} \boldsymbol{B}_1 + \cdots$ and imposing a solvability condition for the \boldsymbol{B}_1 equation yields

$$\boldsymbol{B}^{\varepsilon} = \gamma_0 \varepsilon^{2s-1} \boldsymbol{\xi}_s + O(\varepsilon^{2(2s-1)}), \qquad \gamma_0 = \frac{2\mathfrak{a}_s}{N \bar{l}_s \mathfrak{b}_s} \frac{\boldsymbol{l}_s^T \boldsymbol{e}_N}{\boldsymbol{l}_s^T \boldsymbol{\xi}_s}.$$

The preceding discussion implies that our asymptotic expansion is consistent with the assumption $V_i^{\varepsilon}(X) \gg \varepsilon^{2s}$ that we made to neglect the inhomogeneous term on the right-hand side of (2.15).

Remark 2.2. Since $\mathbf{B}^{\varepsilon} = O(\varepsilon^{2s-1})$ for all 0 < s < 1, we deduce from (2.5a) that $\chi^{\varepsilon} = O(\varepsilon^{2s-1})$ for s < 1/2 and $\chi^{\varepsilon} = O(\log(1/\varepsilon))$ for s = 1/2, whereas $\chi^{\varepsilon} = O(1)$ for 1/2 < s < 1. Hence, (2.5c) implies that to leading order the MFHT in the outer region is spatially constant for $s \le 1/2$, whereas it is spatially variable for 1/2 < s < 1.

Remark 2.3. If the target configuration is symmetric, in the sense that $l_1 = \cdots = l_N = l$ and adjacent targets are equidistant, then $\nu_1 = \cdots = \nu_N = \nu$, the Green's matrix \mathcal{G}_s is circulant, $\mathcal{L}_s = l\mathcal{I}_N$, and $\mathcal{N}^\varepsilon = \nu\mathcal{I}_N$. The solution to (2.5b) is then explicitly given by $\mathbf{B}^\varepsilon = \frac{2\mathbf{a}_s\varepsilon^{2s-1}}{Nlb_s}\mathbf{e}_N$ and $\mathbf{B}^\varepsilon = \frac{2}{\pi N}\mathbf{e}_N$ for $s \neq 1/2$ and s = 1/2, respectively. Moreover, it suffices to consider symmetric configurations for only N = 1 since the case N > 1 can be obtained by a simple spatial rescaling.

2.4. Probability distribution for $s \in (0, 1/2]$. We now extend the preceding analysis of the MFHT to obtain the full probability distribution of the FHT in the limit $\varepsilon \to 0$ for $s \in (0, 1/2]$. The *m*th moment of the FHT,

$$v_m(x) := \mathbb{E}[\tau^m \mid X(0) = x], \quad m \in \{1, 2, \dots\},$$

satisfies the following fractional equation, which couples to the (m-1) moment (see Appendix B),

$$(2.22) \qquad (-\Delta)^s v_m = m v_{m-1},$$

with identical boundary conditions to the first moment and $v_1 = v$. For the m = 2 moment, this becomes

$$(2.23) (-\Delta)^s v_2 = 2v_1.$$

For $s \in (0,1/2]$, we have shown that $v_1(x)$ is constant in space to leading order, $v_1(x) \sim \mu_{s,\varepsilon}$. Dividing (2.23) by twice this constant implies that $w_2 := v_2/(2\mu_{s,\varepsilon})$ satisfies the same fractional equation as the first moment v_1 to leading order. Hence, $w_2 \sim v_1$ and thus $v_2 \sim 2(v_1)^2$. Continuing this argument yields the leading order behavior of the mth moment,

$$v_m \sim m!(v_1)^m, \quad m \in \{1, 2, \dots\},\$$

which implies that $\tau/\mu_{s,\varepsilon}$ is exponentially distributed with unit mean in the limit $\varepsilon \to 0$ (since exponential random variables are determined by their moments [6]).

- 3. Numerical simulations. In this section, we numerically calculate the FHT by solving the fractional differential equation (1.9) directly, as well as by using Monte Carlo methods. These numerical calculations will serve the purpose of validating the formal asymptotic calculations of the previous section, with the Monte Carlo simulations also allowing us to investigate the full probability distribution of the FHT. We proceed by first outlining the numerical methods used to solve (1.9) in section 3.1. In section 3.2, we outline the methods used in the Monte Carlo simulations. Finally, in section 3.3 we showcase the results from our numerical computations.
- 3.1. Solving the MFHT fractional differential equation. To numerically solve (1.9), we require only a numerical discretization of the periodic fractional Laplacian $(-\Delta)^s$. Our numerical discretization of the periodic fractional Laplacian is based on the finite difference–quadrature approach of Huang and Oberman [26]. Fix an integer M > 0, let h = 2/M, and let

$$(3.1) z_n = -1 + hn, n \in \mathcal{M} := \{0, \dots, M - 1\},$$

be a uniform discretization of the interval -1 < x < 1. Denote by $(-\Delta_h)^s$ the numerical discretization of the periodic fractional Laplacian on -1 < x < 1. The discrete operator $(-\Delta_h)^s$ acts on an arbitrary vector $\boldsymbol{\varphi} = (\varphi_0, \dots, \varphi_{M-1})^T$ according to (see equation (FL_h) in [26])

$$(3.2) \quad ((-\Delta_h)^s \boldsymbol{\varphi})_n = \sum_{m \in \mathcal{M}} (\varphi_n - \varphi_m) W_{n-m}, \quad W_{\sigma} := w_{\sigma} + \sum_{k=1}^{\infty} (w_{\sigma-kM} + w_{\sigma+kM}),$$

where we have used periodicity to simplify the expression and where each w_m ($m \in \mathbb{Z}$) is an appropriately chosen weight. See Appendix A for additional details on our choice

of weights, as well as some practical considerations for their computation. Define the set $\mathscr{I} := \{n \in \mathscr{M} \mid z_n \in \bigcup_{i=1}^N (x_i - \varepsilon l_i, x_i + \varepsilon l_i)\}$. The numerical solution to the hitting-time problem (1.9) is then obtained by finding $\boldsymbol{v} = (v_0, \dots, v_{M-1})^T$ satisfying linear system

(3.3)
$$\begin{cases} \sum_{m \in \mathcal{M} \setminus \mathcal{I}} (v_n - v_m) W_{n-m} = 1, & n \in \mathcal{M} \setminus \mathcal{I}, \\ v_n = 0, & n \in \mathcal{I}. \end{cases}$$

In section 3.3, we use M = 50,000 points and K = 10,000 terms in the evaluation of the weights W_{σ} (see (A.3) in Appendix A) and solve the resulting symmetric linear systems using the conjugate gradient routine in the SciPy Python library.

3.2. Monte Carlo. We now describe the stochastic simulation algorithm used to generate FHTs of Lévy flights. Our stochastic simulation algorithm relies on constructing a Lévy fight by subordinating a Brownian motion [33]. Specifically, let $B = \{B(u)\}_{u\geq 0}$ be a one-dimensional Brownian motion with unit diffusivity (i.e., scaled so that $\mathbb{E}[(B(u))^2] = 2u$ for all $u \geq 0$), and let $U = \{U(t)\}_{t\geq 0}$ be an independent s-stable Lévy subordinator (i.e., it has Laplace exponent $\Phi(\beta) = \beta^s$). Then, the following random time change of B,

(3.4)
$$X(t) := D_s^{1/(2s)} B(U(t)), \quad t \ge 0,$$

is a Lévy flight with generalized diffusivity $D_s > 0$.

Given a discrete time step $\Delta t > 0$, we construct a statistically exact path of the s-stable subordinator $\{U(t)\}_{t\geq 0}$ on the discrete time grid $\{t_k\}_{k\in\mathbb{N}}$ with $t_k = k\Delta t$ via

$$U(t_{k+1}) = U(t_k) + (\Delta t)^{1/s} \Theta_k, \quad k \ge 0,$$

where $U(t_0) = U(0) = 0$ and $\{\Theta_k\}_{k \in \mathbb{N}}$ is an i.i.d. sequence of realizations of [13]

$$\Theta = \frac{\sin(s(V + \pi/2))}{(\cos(V))^{1/s}} \left(\frac{\cos(V - \gamma(V + \pi/2))}{E}\right)^{(1-s)/s},$$

where V is uniformly distributed on $(-\pi/2, \pi/2)$ and E is an independent exponential random variable with $\mathbb{E}[E] = 1$. We then construct a statistically exact path of the Brownian motion $\{B(u)\}_{u\geq 0}$ on the (random) discrete time grid $\{U(t_k)\}_{k\in\mathbb{N}}$ via

$$B(U(t_{k+1})) = B(U(t_k)) + \sqrt{2(\Delta t)^{1/s}\Theta_k \xi_k}, \quad k \ge 0,$$

where $\{\xi_k\}_{k\in\mathbb{Z}}$ is an i.i.d. sequence of standard Gaussian random variables and we impose periodic boundary conditions. Finally, we obtain a statistically exact path of the Lévy flight $X=\{X(t)\}_{t\geq 0}$ in (3.4) on the discrete time grid $\{t_k\}_{k\in\mathbb{N}}$ via $X(t_k)=D_s^{1/(2s)}B(U(t_k))$ for $k\geq 0$. The FHT τ to the target set U_{target} is then approximated by $\tau\approx \overline{k}\Delta t$, where $\overline{k}:=\min\{k\Delta t\geq 0: X(t_k)\in U_{\text{target}}\}$.

The Monte Carlo data in the results below is computed from 10^3 independent trials with $\Delta t = 10^{-5}$ and $D_s = 1$.

3.3. Results. To validate our asymptotic analysis, we compare our asymptotic approximations for the MFHT with full numerical simulations using the methods outlined in sections 3.1 and 3.2. We present this comparison for two types of configurations. The first, which we refer to as the *symmetric one-target configuration*,

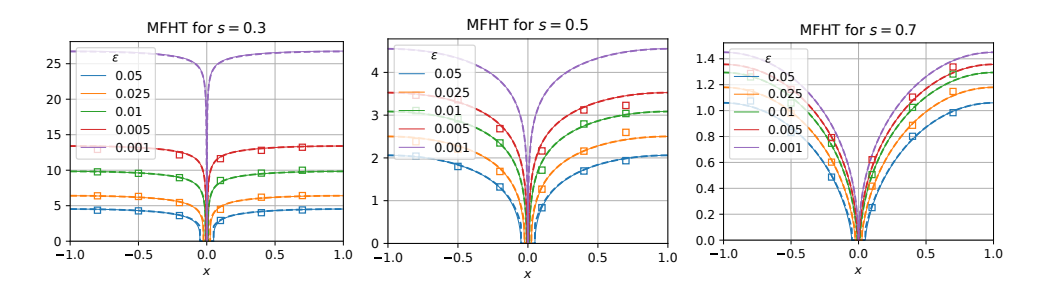


FIG. 2. MFHT for the symmetric one-target configuration. Solid curves, dashed curves, and hollow squares correspond to solutions obtained by numerically solving the fractional PDE (1.9), by using the asymptotic approximations (2.5c), and from Monte Carlo simulations, respectively.

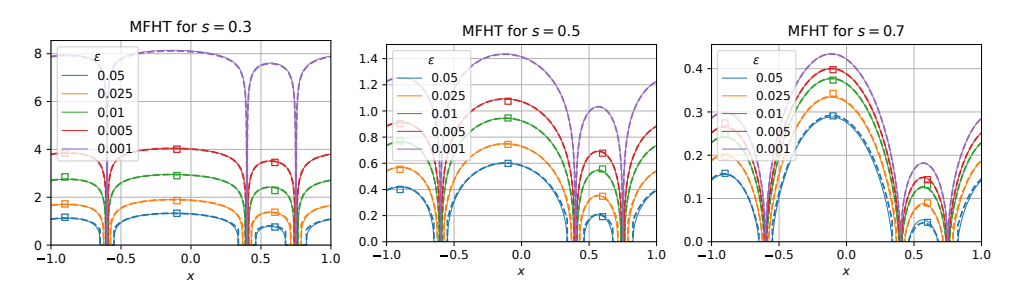


Fig. 3. MFHT for the asymmetric three-target configuration. Solid curves, dashed curves, and hollow squares correspond to solutions obtained by numerically solving the fractional differential equation (1.9), by using the asymptotic approximations (2.5c), and from Monte Carlo simulations, respectively.

consists of a single target with $x_1 = 0$ and $l_1 = 1$. The second, which we refer to as the asymmetric three-target configuration, consists of N = 3 targets centered at $x_1 = -0.6$, $x_2 = 0.4$, and $x_3 = 0.75$ with $l_1 = 1$, $l_2 = 1.25$, and $l_3 = 1.5$.

In Figures 2 and 3, we plot the MFHT for the symmetric one-target and asymmetric three-target configurations, respectively. Specifically, each figure compares the solution obtained by solving (1.9) numerically (solid curves), the solution obtained using the asymptotic approximation (2.5c) (dashed curves), and the values of the MFHT starting from specific values of $x \in (-1,1)$ obtained from Monte Carlo simulations (hollow squares). In each case, we observe excellent agreement between the asymptotic and numerical solutions even for moderately sized values of $\varepsilon > 0$. In addition to validating our asymptotic approximations, the plots in Figures 2 and 3 also showcase the qualitative properties of the MFHT predicted by our asymptotic analysis. Specifically, they illustrate a strong ε -dependence when s < 1/2 in contrast to when s > 1/2 which supports the scaling $v = O(\varepsilon^{2s-1})$ for s < 1/2 and v = O(1) for s>1/2. Moreover, we observe that for sufficiently small values of $\varepsilon>0$, the MFHT in the outer region is approximately spatially constant when s < 1/2, whereas it is spatially variable when s > 1/2. Although the leading order asymptotics predict a spatially constant solution for s = 1/2, this is difficult to see numerically since the first order correction is $O(1/\log \varepsilon)$.

An additional quantity of interest is the MFHT averaged over uniformly distributed initial points $x \in (-1,1)$, i.e.,

$$\overline{v} := \frac{1}{2} \int_{-1}^{1} v(x) dx.$$

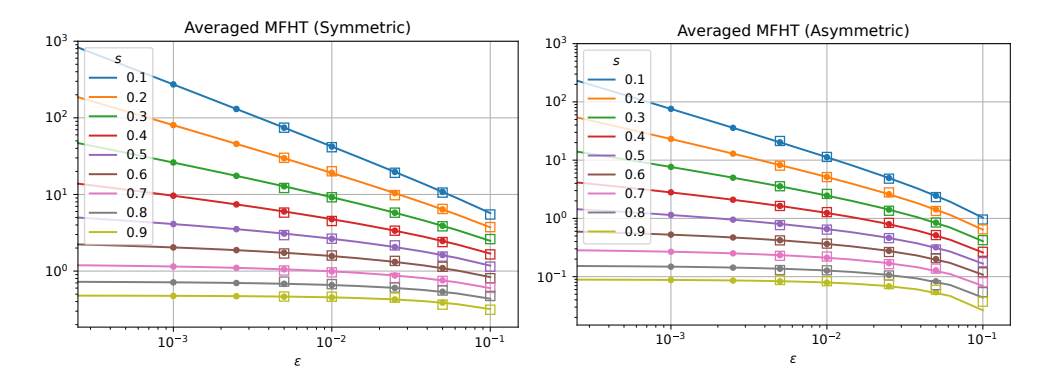


FIG. 4. The MFHT averaged over a uniformly distributed initial condition in $\Omega \setminus \Omega_{target}$ for the (left) symmetric one-target configuration and the (right) asymmetric three-target configuration. In each plot, the solid curve indicates the asymptotic approximation, the dots indicate results from numerically solving the fractional differential equation (1.9), and the hollow squares indicate those values obtained by stochastic simulations.

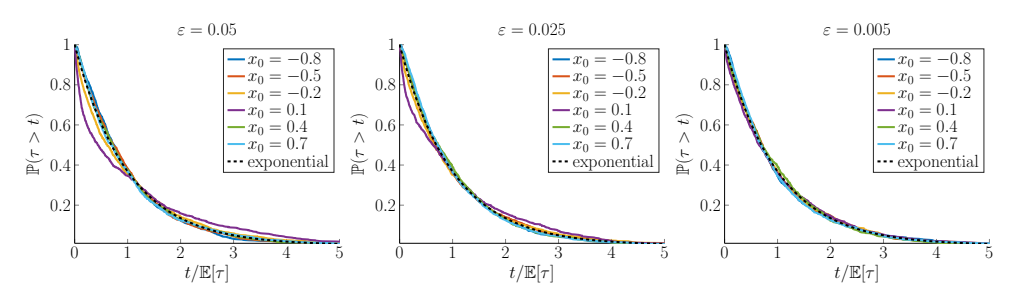


Fig. 5. Probability distribution of FHT.

In Figure 4, we plot this averaged MFHT versus $\varepsilon > 0$ for different values of 0 < s < 1 for both the symmetric one-target and the asymmetric three-target configurations. In each plot, the solid curve corresponds to the asymptotically computed solution which, in light of the vanishing integral constraint in (2.12), is equal to χ^{ε} given by (2.5a). The solid dots correspond to values obtained by numerically integrating the numerical solution to (1.9), whereas the hollow squares are results from Monte Carlo simulations. These plots shows good agreement between the asymptotic approximation and numerical simulations.

Finally, in Figure 5, we compare (i) the full probability distribution of the FHT τ computed from stochastic simulations to (ii) the exponential distribution implied by the analysis in section 2.4. This plot is for the symmetric one-target configuration in Figure 2 with s=0.3. The convergence to an exponential distribution is apparent as ε decreases from $\varepsilon=0.05$ in the left panel down to $\varepsilon=0.005$ in the right panel.

4. Optimal random search. We now investigate the value of the fractional order $s \in (0,1]$ which minimizes the averaged MFHT. By averaging over a uniformly distributed initial position, considering the case N=1, neglecting the highest order terms from our asymptotic expansion, and reversing the nondimensionalization in (1.7), we arrive at the following dimensional measure of the search time:

$$T_s := \begin{cases} (l^{2s}/D_s)(\varepsilon^{2s-1} 2\mathfrak{a}_s/\mathfrak{b}_s - 2\mathfrak{a}_s R_s(0)) & \text{if } s \neq 1/2, \\ (l^{2s}/D_s)(\log(2/\varepsilon)2/\pi - 2R_{1/2}(0)/\pi) & \text{if } s = 1/2 \end{cases}$$
 for $s \in (0,1)$.

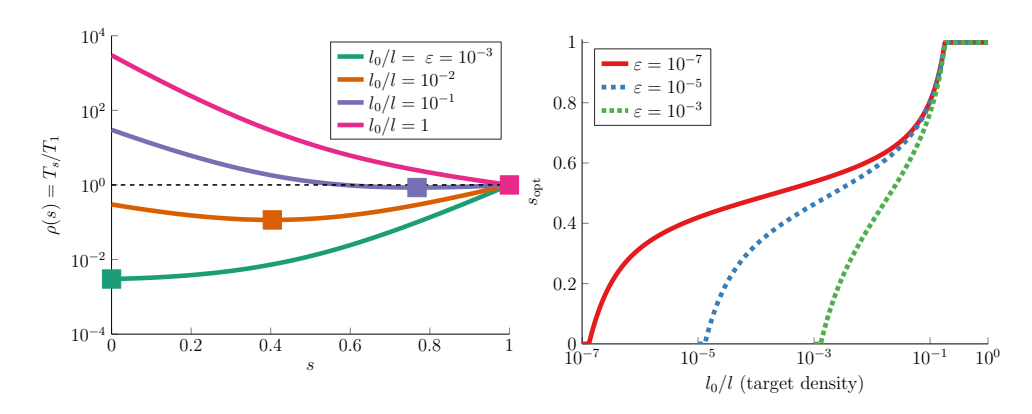


FIG. 6. (left) $\rho(s)$ in (4.1) as a function of $s \in (0,1)$ for $\varepsilon = 10^{-3}$ and different values of the target density l_0/l . Square markers indicate s_{opt} in (4.2). (right) s_{opt} as a function of the target density l_0/l for different values of ε .

That is, T_s is the averaged MFHT over uniformly distributed initial positions of a one-dimensional, (2s)-stable Lévy flight with generalized diffusivity $D_s > 0$ and an infinite periodic array of targets with separation distance 2l > 0 where each target has radius εl with $0 < \varepsilon \ll 1$.

To study how T_s depends on $s \in (0,1]$, we must choose how the generalized diffusivity D_s depends on s (since it has dimension $[D_s] = (\text{length})^{2s}/(\text{time})$). We follow [50] and introduce a lengthscale $l_0 > 0$ (independent of s) and suppose

$$D_s = (l_0)^{2s}/t_0$$

for some timescale t_0 . Such a lengthscale $l_0 > 0$ arises naturally in the continuous-time random walk derivation of a Lévy flight (see (1.3)–(1.6) in section 1 and [42] for more details). Normalizing T_s by the Brownian search time $T_1 := (l^2/D_1)(1-\varepsilon)^2/3$ yields the following ratio for $s \in (0,1)$:

(4.1)
$$\rho(s) := \frac{T_s}{T_1} = \frac{(l_0/l)^{2(1-s)}}{(1-\varepsilon)^2/3} \times \begin{cases} \varepsilon^{2s-1} 2\mathfrak{a}_s/\mathfrak{b}_s - 2\mathfrak{a}_s R_s(0) & \text{if } s \neq 1/2, \\ \log(2/\varepsilon)2/\pi - 2R_{1/2}(0)/\pi & \text{if } s = 1/2. \end{cases}$$

Hence, $\rho(s) < 1$ (respectively, $\rho(s) > 1$) means that the Lévy search is faster (respectively, slower) than Brownian search.

In the left panel of Figure 6, we plot $\rho(s)$ as a function of $s \in (0,1)$ for different values of l_0/l . Notice that $l_0/l \ll 1$ describes sparse targets and $l_0/l \ll 1$ describes dense targets (where "sparse" and "dense" are relative to the lengthscale l_0). This plot shows that Lévy search is faster than Brownian search for sparse targets, whereas Brownian search is faster than Lévy search for dense targets.

In the right panel of Figure 6, we plot the "optimal" value of $s \in (0,1]$ which minimizes the search time,

$$(4.2) s_{\text{opt}} := \arg\min_{s} \rho(s),$$

as a function of the target density l_0/l for fixed values of ε . This plot shows that $s_{\rm opt}$ varies continuously from $s_{\rm opt} \approx 0$ for sparse targets up to $s_{\rm opt} \approx 1$ (i.e., Brownian search) as the target density increases. Hence, the value s=1/2 (which corresponds to stability index $\alpha=2s=1$, i.e., so-called inverse square Lévy search) is not distinguished from other values of $s\in (0,1]$ in the sense that $s_{\rm opt}=1/2$ for only a single

value of the target density l_0/l for each $\varepsilon>0$. To further emphasize this point, observe that treating l_0/l and ε as independent variables we deduce $\lim_{\varepsilon\to 0}\lim_{l/l_0\to 0}s_{\rm opt}=0$, whereas $\lim_{l/l_0\to 0}\lim_{\varepsilon\to 0}s_{\rm opt}=1/2$. The former follows from noting that $(l_0/l)^{2(1-s)}$ is minimized at s=0 for any $l_0/l\ll 1$. To deduce the latter, note first that we must have $\lim_{\varepsilon\to 0}s_{\rm opt}>1/2$ since (4.1) implies $\lim_{\varepsilon\to 0}\rho(s)=+\infty$ if $s\le 1/2$. Next, (4.1) implies

$$\lim_{s \to 0} \rho(s) = -((l_0/l)^{2(1-s)}/3)(2\mathfrak{a}_s R_s(0)) > 0 \quad \text{if } s > 1/2,$$

and therefore $\lim_{l_0/l\to 0}\lim_{\varepsilon\to 0}s_{\rm opt}=1/2$. Since the limiting value of $s_{\rm opt}$ depends on the order in which we take $\varepsilon\to 0$ and $l/l_0\to 0$, we deduce that details of the configuration's target size and density must be considered to draw quantitative conclusions about the optimal value $s_{\rm opt}$.

5. Discussion. In this paper, we calculated an asymptotic approximation for the MFHT to a small target in a periodic one-dimensional domain. Our asymptotic approximation is summarized in Principal Result 1 and reduces the calculation of the MFHT to that of solving the linear system (2.5b), thereby providing a fast method for approximating the MFHT when the target size is small. In the special case of a symmetric configuration, it suffices to consider the case of a single target for which the system (2.5b) can be solved explicitly (see (1.10)–(1.13) in section 1). Furthermore, we validated our asymptotics by comparing them to numerical computations of the MFHT obtained by solving the fractional differential equation (1.9) directly and by using stochastic simulations.

The asymptotic analysis leading to Principal Result 1 is analogous to that used in two- and three-dimensional narrow capture/escape problems involving pure diffusion [55, 16]. This analogy was previously identified in [21, 22] and is a result of the singular behavior of the fractional free-space Green's function which is logarithmic when s=1/2 and algebraic when s<1/2, mirroring that of the classical free-space Green's function in two and three dimensions, respectively. A novel aspect of the asymptotic analysis presented in this paper is the recognition of a fractional counterpart to the classical electrified disk problem. This fractional differential equation was solved by using a fractional Kelvin transform and fractional Poisson kernel for $s\neq 1/2$ and by considering a two-dimensional extended problem solvable by complex analysis methods for s=1/2. In addition, we determined that when $s\leq 1/2$ the MFHT is spatially constant to leading order, with this observation further allowing us to conclude that the FHT is exponentially distributed when $s\leq 1/2$.

The present study joins many prior works which use Lévy flights as simple theoretical models to investigate optimal search strategies. Prior works often choose one-dimensional spatial domains due to their analytical tractability and as models for search in effectively one-dimensional domains such as in streams, along coastlines, at forest-meadows, and in other borders [50, 32, 49, 51, 48, 45, 47]. The very interesting work of Palyulin, Chechkin, and Metzler [50] is perhaps most closely related to our present study. In [50], the authors consider a one-dimensional, possibly biased Lévy flight on the entire real line with a single point-like target. A major result of [50] is that despite the frequent claim that Lévy flights with s=1/2 are most efficient for sparse targets, the optimal value of s may range the entire interval between s=1/2 and s=1 and thus include Brownian search (the assumption of a point-like target in [50] meant that these authors did not consider s=1/2. Indeed, as the authors of [50] state, "the main message from this study is that Lévy flight search and its optimization is sensitive to the exact conditions" and "our results show clear limitations

for the universality of Lévy flight foraging" [50]. Our results agree with these main points, as the optimal value of s in our study spans the entire interval (0,1] as the target density l_0/l increases from $l_0/l \le \varepsilon$ up to $l_0/l \approx 1$ (see Figure 6).

Appendix A. Additional considerations for the numerical discretization of the periodic fractional Laplacian. To numerically implement (3.3), we choose weights w_n ($n \in \mathbb{Z}$) that are based on linear interpolants. Specifically, we define (see section 3.1 of [26])

(A.1)
$$F(t) := \begin{cases} \frac{C_s}{2s(2s-1)} |t|^{1-2s}, & s \neq 1/2, \\ -C_s \log |t|, & s = 1/2, \end{cases}$$

where C_s is given by (1.5) and in terms of which the weights are given by

(A.2)
$$w_n := \frac{1}{h^{2s}} \begin{cases} \frac{C_s}{2 - 2s} - F'(1) + F(2) - F(1), & |n| = 1, \\ F(n+1) - 2F(n) + F(n-1), & |n| \ge 2. \end{cases}$$

We use the explicit form of the weights to numerically speed up the evaluation of the infinite sums appearing in the definition of W_{σ} in (3.2). For sufficiently large $n \in \mathbb{Z}$, we have

$$w_n = \frac{C_s}{h^{2s}|n|^{1+2s}} \left(1 + O\left(\frac{1}{n^4}\right)\right),$$

so that for any fixed $\sigma \in \mathbb{Z}$ and any sufficiently large integer $k \geq 1$ we have

$$w_{\sigma-kM} + w_{\sigma+kM} = \frac{C_s}{2^{2s-1}Mk^{1+2s}} \left(1 + O\left(\left(\frac{\sigma}{kM} \right)^2 \right) \right).$$

Choosing a sufficiently large integer $K \geq 1$, we obtain

(A 3)

$$W_{\sigma} = w_{\sigma} + \sum_{k=1}^{K} (w_{\sigma-kM} + w_{\sigma+kM}) + \frac{C_s}{2^{2s-1}M} \zeta(1+2s, K+1) + O\left(\frac{\sigma^2}{M^3 K^{2+2s}}\right),$$

where $\zeta(z,q) := \sum_{n=0}^{\infty} (n+q)^{-z}$ is the Hurwitz zeta function which can be quickly computed by standard numerical libraries. This formula for the weights W_{σ} ($\sigma \in \mathbb{Z}$) provides a good approximation for W_{σ} for moderately sized K, thereby reducing computational costs.

Appendix B. Derivation of fractional equations for FHT moments. Let p(y,t|z,u) denote the conditional probability density that X(t)=y given that X(u)=z for $0 \le u \le t$. Since X is a Markov process, its density satisfies the Chapman–Kolmogorov equation [52],

$$(\mathrm{B.1}) \qquad \quad p(y,t|z,0) = \int p(y,t|x,u) p(x,u|z,0) \, \mathrm{d}x \quad \text{for any } 0 \leq u \leq t.$$

Differentiating (B.1) with respect to the intermediate time u and using the forward Fokker–Planck equation in (1.4) yields

$$0 = \int p(y,t|x,u) \frac{\partial}{\partial u} p(x,u|z,0) \, dx + \int p(x,u|z,0) \frac{\partial}{\partial u} p(y,t|x,u) \, dx$$
$$= -D_s \int p(y,t|x,u) (-\Delta_x)^s p(x,u|z,0) \, dx + \int p(x,u|z,0) \frac{\partial}{\partial u} p(y,t|x,u) \, dx,$$

where $-(-\Delta_x)^s$ denotes the fractional Laplacian acting on x. Since the fractional Laplacian is self-adjoint, we then obtain

$$0 = \int p(x, u|z, 0) \left(\frac{\partial}{\partial u} p(y, t|x, u) - D_s(-\Delta_x)^s p(y, t|x, u) \right) dx.$$

Taking $u \to 0$ and using that $p(x,0|z,0) = \delta(z-x)$ and $\frac{\partial}{\partial u}p(y,t|x,u) = -\frac{\partial}{\partial t}p(y,t-u|x,0)$ yields the backward Fokker–Planck (or backward Kolmogorov) equation,

(B.2)
$$\frac{\partial}{\partial t}p(y,t|x,0) = -D_s(-\Delta_x)^s p(y,t|x,0).$$

The survival probability of the FHT τ conditioned that X(0) = x can be written in terms of the density,

$$\mathbb{P}(\tau > t \,|\, X(0) = x) = \int p(y, t | x, 0) \,\mathrm{d}y.$$

Now, the mth moment of any nonnegative random variable T is [20]

$$\mathbb{E}[T^m] = \int_0^\infty \mathbb{P}(T^m > a) \, \mathrm{d}a = \int_0^\infty m t^{m-1} \mathbb{P}(T > t) \, \mathrm{d}t,$$

where the final equality follows from changing variables. Therefore,

$$v_m(x) = \mathbb{E}[\tau^m \mid X(0) = x] = \int_0^\infty mt^{m-1} \int p(y, t \mid x, 0) \, dy \, dt.$$

Taking the fractional Laplacian with respect to x, using (B.2), and integrating by parts yields

$$-D_s(-\Delta_x)^s v_m(x) = \int_0^\infty m t^{m-1} \int \frac{\partial}{\partial t} p(y, t|x, 0) \, \mathrm{d}y \, \mathrm{d}t$$

$$= \left(m t^{m-1} \int p(y, t|x, 0) \, \mathrm{d}y \right) \Big|_0^\infty$$

$$- m \int_0^\infty (m-1) t^{m-2} \int p(y, t|x, 0) \, \mathrm{d}y \, \mathrm{d}t.$$

If m = 1, then the integral term in (B.3) vanishes and we obtain the fractional equation in (1.9). If m > 1, then the boundary terms vanish and we obtain (2.22). The result that v_m satisfies the boundary conditions in (1.9) is immediate.

REFERENCES

- [1] N. ABATANGELO AND E. VALDINOCI, Getting acquainted with the fractional Laplacian, in Contemporary Research in Elliptic PDEs and Related Topics, Springer, Cham, 2019, pp. 1–105.
- [2] H. AMMARI, J. GARNIER, H. KANG, H. LEE, AND K. SØLNA, The mean escape time for a narrow escape problem with multiple switching gates, Multiscale Model. Simul., 9 (2011), pp. 817–833, https://doi.org/10.1137/100817103.
- [3] O. Benichou, D. Grebenkov, P. Levitz, C. Loverdo, and R. Voituriez, Optimal reaction time for surface-mediated diffusion, Phys. Rev. Lett., 105 (2010), 150606, https://doi.org/10.1103/PhysRevLett.105.150606.
- [4] O. BÉNICHOU, C. LOVERDO, M. MOREAU, AND R. VOITURIEZ, Intermittent search strategies, Rev. Mod. Phys., 83 (2011), 81.
- [5] J. BERTOIN, Lévy Processes, Cambridge Tracts in Math. 121, Cambridge University Press, Cambridge, UK, 1996.

- [6] P. Billingsley, Probability and Measure, John Wiley & Sons, New York, 2008.
- [7] R. M. BLUMENTHAL, R. K. GETOOR, AND D. RAY, On the distribution of first hits for the symmetric stable processes, Trans. Amer. Math. Soc., 99 (1961), pp. 540-554.
- [8] P. C. Bressloff and S. D. Lawley, Mean first passage times for piecewise deterministic Markov processes and the effects of critical points, J. Stat. Mech. Theory Exp., 2017 (2017), 063202.
- P. C. Bressloff and R. D. Schumm, The narrow capture problem with partially absorbing targets and stochastic resetting, Multiscale Model. Simul., 20 (2022), pp. 857–881, https://doi.org/10.1137/21M1449580.
- [10] C. Bucur, Some observations on the Green function for the ball in the fractional Laplace framework, Commun. Pure Appl. Anal., 15 (2016), pp. 657–699, https://doi.org/10.3934/cpaa.2016.15.657.
- [11] S. BULDYREV, E. RAPOSO, F. BARTUMEUS, S. HAVLIN, F. RUSCH, M. DA LUZ, AND G. VISWANATHAN, Comment on "Inverse square Lévy walks are not optimal search strategies for d≥2," Phys. Rev. Lett., 126 (2021), 048901.
- [12] L. CAFFARELLI AND L. SILVESTRE, An extension problem related to the fractional Laplacian, Comm. Partial Differential Equations, 32 (2007), pp. 1245–1260.
- [13] S. CARNAFFAN AND R. KAWAI, Solving multidimensional fractional Fokker-Planck equations via unbiased density formulas for anomalous diffusion processes, SIAM J. Sci. Comput., 39 (2017), pp. B886-B915, https://doi.org/10.1137/17M111482X.
- [14] Y. CHAUBET, T. LEFEUVRE, Y. G. BONTHONNEAU, AND L. TZOU, Geodesic Levy Flights and Expected Stopping Time for Random Searches, preprint, arXiv:2211.13973, 2022.
- [15] A. V. CHECHKIN, R. METZLER, V. Y. GONCHAR, J. KLAFTER, AND L. V. TANATAROV, First passage and arrival time densities for Lévy flights and the failure of the method of images, J. Phys. A, 36 (2003), pp. L537–L544.
- [16] A. F. CHEVIAKOV, M. J. WARD, AND R. STRAUBE, An asymptotic analysis of the mean first passage time for narrow escape problems: Part II: The sphere, Multiscale Model. Simul., 8 (2010), pp. 836–870, https://doi.org/10.1137/100782620.
- [17] T. CHOU AND M. R. D'ORSOGNA, First passage problems in biology, in First-Passage Phenomena and Their Applications, World Scientific, Hackensack, NJ, 2014, pp. 306–345.
- [18] DIGITAL LIBRARY OF MATHEMATICAL FUNCTIONS, F. W. J. OLVER, A. B. OLDE DAALHUIS, D. W. LOZIER, B. I. SCHNEIDER, R. F. BOISVERT, C. W. CLARK, B. R. MILLER, B. V. SAUNDERS, H. S. COHL, AND M. A. MCCLAIN, EDS., http://dlmf.nist.gov/, Release 1.0.28 of 2020-09-15.
- [19] A. A. Dubkov, B. Spagnolo, and V. V. Uchaikin, Lévy flight superdiffusion: An introduction, Internat. J. Bifur. Chaos Appl. Sci. Engrg., 18 (2008), pp. 2649–2672.
- [20] R. DURRETT, Probability: Theory and Examples, Cambridge University Press, Cambridge, UK, 2019.
- [21] D. GOMEZ, M. DE MEDEIROS, J.-C. WEI, AND W. YANG, Spike solutions to the supercritical fractional Gierer-Meinhardt system, J. Nonlinear Sci., 34, 24 (2024).
- [22] D. Gomez, J. Wei, and Z. Yang, Multi-spike solutions to the one-dimensional subcritical fractional Schnakenberg system, Phys. D, 448 (2023), 133720, https://doi.org/10.1016/j.physd.2023.133720.
- [23] D. S. Grebenkov and G. Oshanin, Diffusive escape through a narrow opening: New insights into a classic problem, Phys. Chem. Phys., 19 (2017), pp. 2723–2739.
- [24] B. GUINARD AND A. KORMAN, Intermittent inverse-square Lévy walks are optimal for finding targets of all sizes, Sci. Adv., 7 (2021), eabe8211.
- [25] D. HOLCMAN AND Z. SCHUSS, The narrow escape problem, SIAM Rev., 56 (2014), pp. 213–257, https://doi.org/10.1137/120898395.
- [26] Y. Huang and A. Oberman, Numerical methods for the fractional Laplacian: A finite difference-quadrature approach, SIAM J. Numer. Anal., 52 (2014), pp. 3056–3084, https://doi.org/10.1137/140954040.
- [27] P. Jolakoski, A. Pal, T. Sandev, L. Kocarev, R. Metzler, and V. Stojkoski, The Fate of the American Dream: A First Passage under Resetting Approach to Income Dynamics, preprint, arXiv:2212.13176, 2022.
- [28] J. KAYE AND L. GREENGARD, A fast solver for the narrow capture and narrow escape problems in the sphere, J. Comput. Phys. X, 5 (2020), 100047.
- [29] T. Koren, A. Chechkin, and J. Klafter, On the first passage time and leapover properties of Lévy motions, Phys. A, 379 (2007), pp. 10-22.
- [30] T. KOREN, M. A. LOMHOLT, A. V. CHECHKIN, J. KLAFTER, AND R. METZLER, Leapover lengths and first passage time statistics for Lévy flights, Phys. Rev. Lett., 99 (2007), 160602.

- [31] V. Kurella, J. C. Tzou, D. Coombs, and M. J. Ward, Asymptotic analysis of first passage time problems inspired by ecology, Bull. Math. Biol., 77 (2015), pp. 83–125.
- [32] L. KUŚMIERZ AND E. GUDOWSKA-NOWAK, Optimal first-arrival times in Lévy flights with resetting, Phys. Rev. E (3), 92 (2015), 052127.
- [33] S. D. LAWLEY, Extreme statistics of superdiffusive Lévy flights and every other Lévy subordinate Brownian motion, J. Nonlinear Sci., 33 (2023), 53.
- [34] S. D. LAWLEY AND J. JOHNSON, Why is there an "oversupply" of human ovarian follicles?, Biol. Reprod., 108 (2023), pp. 814–821.
- [35] N. LEVERNIER, J. TEXTOR, O. BÉNICHOU, AND R. VOITURIEZ, Inverse square Lévy walks are not optimal search strategies for d≥2, Phys. Rev. Lett., 124 (2020), 080601.
- [36] N. LEVERNIER, J. TEXTOR, O. BÉNICHOU, AND R. VOITURIEZ, Reply to "Comment on Inverse square Lévy walks are not optimal search strategies for $d \ge 2$," Phys. Rev. Lett., 126 (2021), 048902.
- [37] A. E. LINDSAY, A. J. BERNOFF, AND M. J. WARD, First passage statistics for the capture of a Brownian particle by a structured spherical target with multiple surface traps, Multiscale Model. Simul., 15 (2017), pp. 74–109, https://doi.org/10.1137/16M1077659.
- [38] A. LISCHKE, G. PANG, M. GULIAN, F. SONG, C. GLUSA, X. ZHENG, Z. MAO, W. CAI, M. M. MEERSCHAERT, M. AINSWORTH, AND G. E. KARNIADAKIS, What is the fractional Laplacian? A comparative review with new results, J. Comput. Phys., 404 (2020), 109009.
- [39] M. A. LOMHOLT, T. AMBJÖRNSSON, AND R. METZLER, Optimal target search on a fast-folding polymer chain with volume exchange, Phys. Rev. Lett., 95 (2005), 260603.
- [40] M. A. LOMHOLT, K. TAL, R. METZLER, AND K. JOSEPH, Lévy strategies in intermittent search processes are advantageous, Proc. Natl. Acad. Sci. USA, 105 (2008), pp. 11055–11059.
- [41] M. M. MEERSCHAERT AND A. SIKORSKII, Stochastic Models for Fractional Calculus, De Gruyter Stud. Math. 43, De Gruyter, Berlin, 2011.
- [42] R. METZLER AND J. KLAFTER, The restaurant at the end of the random walk: Recent developments in the description of anomalous transport by fractional dynamics, J. Phys. A, 37 (2004), pp. R161–R208.
- [43] L. MIRNY, M. SLUTSKY, Z. WUNDERLICH, A. TAFVIZI, J. LEITH, AND A. KOSMRLJ, How a protein searches for its site on DNA: The mechanism of facilitated diffusion, J. Phys. A, 42 (2009), 434013.
- [44] E. W. MONTROLL AND G. H. Weiss, Random walks on lattices, ii, J. Math. Phys., 6 (1965), pp. 167–181.
- [45] A. Padash, A. V. Chechkin, B. Dybiec, M. Magdziarz, B. Shokri, and R. Metzler, First passage time moments of asymmetric lévy flights, J. Phys. A, 53 (2020), 275002.
- [46] A. Padash, A. V. Chechkin, B. Dybiec, I. Pavlyukevich, B. Shokri, and R. Metzler, First-passage properties of asymmetric Lévy flights, J. Phys. A, 52 (2019), 454004.
- [47] A. PADASH, T. SANDEV, H. KANTZ, R. METZLER, AND A. V. CHECHKIN, Asymmetric Lévy flights are more efficient in random search, Fractal Fract., 6 (2022), 260.
- [48] V. V. Palyulin, G. Blackburn, M. A. Lomholt, N. W. Watkins, R. Metzler, R. Klages, and A. V. Chechkin, First passage and first hitting times of Lévy flights and Lévy walks, New J. Phys., 21 (2019), 103028.
- [49] V. V. PALYULIN, A. V. CHECHKIN, R. KLAGES, AND R. METZLER, Search reliability and search efficiency of combined Lévy-Brownian motion: Long relocations mingled with thorough local exploration, J. Phys. A, 49 (2016), 394002.
- [50] V. V. PALYULIN, A. V. CHECHKIN, AND R. METZLER, Lévy flights do not always optimize random blind search for sparse targets, Proc. Natl. Acad. Sci. USA, 111 (2014), pp. 2931– 2936
- [51] V. V. PALYULIN, V. N. MANTSEVICH, R. KLAGES, R. METZLER, AND A. V. CHECHKIN, Comparison of pure and combined search strategies for single and multiple targets, Eur. Phys. J. B, 90 (2017), 170.
- [52] G. A. PAVLIOTIS, Stochastic Processes and Applications: Diffusion Processes, the Fokker-Planck and Langevin Equations, Texts Appl. Math. 60, Springer, New York, 2014.
- [53] I. PAVLYUKEVICH, Lévy flights, non-local search and simulated annealing, J. Comput. Phys., 226 (2007), pp. 1830–1844.
- [54] I. PAVLYUKEVICH, Simulated annealing for Lévy-driven jump-diffusions, Stochastic Process. Appl., 118 (2008), pp. 1071–1105.
- [55] S. PILLAY, M. J. WARD, A. PEIRCE, AND T. KOLOKOLNIKOV, An asymptotic analysis of the mean first passage time for narrow escape problems: Part I: Two-dimensional domains, Multiscale Model. Simul., 8 (2010), pp. 803–835, https://doi.org/10.1137/090752511.
- [56] M. RALF, R. SIDNEY, AND O. GLEB, First-Passage Phenomena and Their Applications, World Sci. Stud. Int. Econ. 35, World Scientific, Singapore, 2014.

- [57] S. REDNER, A Guide to First-Passage Processes, Cambridge University Press, Cambridge, UK, 2001.
- [58] M. REVA, D. A. DIGREGORIO, AND D. S. GREBENKOV, A first-passage approach to diffusioninfluenced reversible binding and its insights into nanoscale signaling at the presynapse, Sci. Rep., 11 (2021), 5377.
- [59] X. ROS-OTON AND J. SERRA, The Dirichlet problem for the fractional Laplacian: Regularity up to the boundary, J. Math. Pures Appl. (9), 101 (2014), pp. 275–302.
- [60] J. TZOU AND L. TZOU, A counterexample to the Lévy flight foraging hypothesis in the narrow capture framework, Phys. Rev. Res., 2024.
- [61] G. VACCARIO, C. ANTOINE, AND J. TALBOT, First-passage times in d-dimensional heterogeneous media, Phys. Rev. Lett., 115 (2015), 240601.
- [62] G. VISWANATHAN, E. RAPOSO, AND M. DA LUZ, Lévy flights and superdiffusion in the context of biological encounters and random searches, Phys. Life Rev., 5 (2008), pp. 133–150.
- [63] G. M. VISWANATHAN, S. V. BULDYREV, S. HAVLIN, M. DA LUZ, E. RAPOSO, AND H. E. STAN-LEY, Optimizing the success of random searches, Nature, 401 (1999), pp. 911–914.
- [64] A. WARDAK, First passage leapovers of Lévy flights and the proper formulation of absorbing boundary conditions, J. Phys. A, 53 (2020), 375001.
- [65] E. M. Wieschen, A. Voss, and S. Radev, Jumping to conclusion? a Lévy flight model of decision making, Quant. Methods Psychol., 16 (2020), pp. 120–132.